

Long-Term Drag Coefficients Measurements in the Coastal Zone

Harry C. Friebel

US Army Corps of Engineers - NAP
Philadelphia, Pennsylvania, USA
Email: Harry.C.Friebel@usace.army.mil

Alexander Y. Benilov
Stevens Institute of Technology
Hoboken, New Jersey, USA

Jeffrey L. Hanson

US Army Corps of Engineers
Duck, North Carolina, USA

Donald T. Resio
US Army Corps of Engineers
Vicksburg, MS, USA

1 Introduction

In an effort to improve the transfer of momentum in nearshore numerical wave modeling, an air-sea momentum flux measurement system was established in October 2005 at the U.S. Army Corps of Engineers Field Research Facility (USACE-FRF) pier located in Duck, NC (Figure 1). The end of the USACE-FRF pier is at approximately 7.5-m depth and extends 560-m into the Atlantic Ocean. Two Gill R3A sonic anemometers and two LI-COR LI-7500 CO_2/H_2O gas analyzers were mounted at the end of the pier on both a boom and tower positioned 10.0 and 16.7-m above mean sea level (MSL), respectively.

Measurements began in October 2005 and continued until October 2007 under a cooperative agreement between the U.S. Army Corps of Engineers, TNO Defence, Security and Safety (TNO) and Lamont-Doherty Earth Observatory (LDEO). In November 2007, the U.S. Army Corps of Engineers retained sole responsibility of the tower measurement system. This report describes tower momentum flux measurements in detail from October 2005 through December 2007 (Figure 2). A description for the boom data collection system can be found in (de Leeuw et al., 2007).

The primary objective of the momentum system is to further understanding of the critical factors influencing drag coefficient behavior in the nearshore during extreme wind events. This is accomplished through the development of a long-term, robust, coastal zone wind stress measurement system that is capable of measuring both tropical and extra-tropical force winds. The momentum system collects direct measurements to determine momentum transfer at the air-sea interface. Drag coefficients are calculated

for wind events greater than 10 m/s to determine dependence on both wind speed and stability and compared to open ocean parameterizations.



Figure 1: U.S. Army Corps of Engineers Field Research Facility pier in Duck, N.C.

2 Theory

The atmospheric planetary boundary layer (PBL) is a region where fluxes are not negligible and on the order of 1 km in height. The lowest 10% (100 m) of the PBL represents the surface boundary layer (SBL) where the turbulent fluxes dominate. Reynolds stresses in the SBL create the logarithmic profile due to shear stresses that slow momentum towards the boundary;

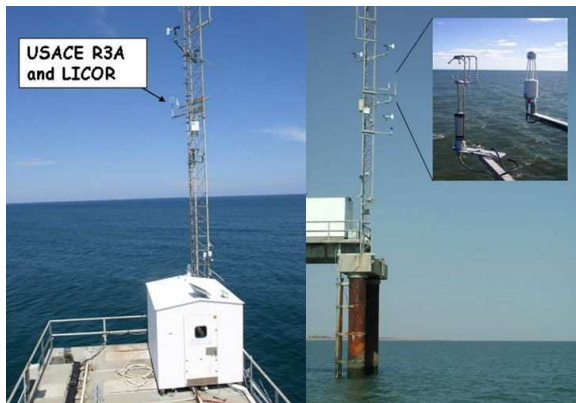


Figure 2: End of the USACE-FRF pier.

$$U_{zN}(z) = \frac{u_*}{\kappa} \ln \frac{z}{z_o} \quad (1)$$

where U_{zN} is the time averaged, neutral stratification, velocity at reference height z , u_* is the friction velocity, $\kappa = 0.4$ is the von Karman constant, and z_o is the roughness length (Prandtl, 1932; Charnock, 1955). The logarithmic wind profile (Equation 1) describing turbulent flow in the boundary layer is only valid well above the aerodynamic roughness length z_o (Monin and Yaglom, 1975). Roughness length is defined as the height where the mean wind speed becomes zero.

Turbulent shear stress (vertical component of horizontal momentum flux) at the surface is defined as;

$$\tau = -\rho (\overline{u'w'}) = \rho u_*^2 \quad (2)$$

$$u_* = \sqrt{-\overline{u'w'}} \quad (3)$$

where ρ is the air density, the over-bar refers to time averaging, u' and w' are the turbulent components of the horizontal and vertical velocities, respectively (Monin and Obukhov, 1954). Within the SBL, the friction velocity is considered constant with height, representing the momentum flux through the air-sea interface.

A requirement for application of the logarithmic wind profile is that neutral atmospheric stability conditions exist. If the underlying ocean surface is colder than the air above, the atmosphere is stable, vertical mixing and momentum transfer is reduced. Conversely, if the atmospheric surface layer is unstable, vertical mixing and turbulent momentum transfer is

enhanced. Atmospheric stability influences the wind velocity to deviate from the logarithmic wind profile (Equation 1).

Monin and Obukhov (1954) introduced a length scale, L , to represent a transition height where convectively driven turbulence governs over mechanically driven turbulence;

$$L = -\frac{u_*^3 T_v}{g k t'_v w} \quad (4)$$

Paulson (1970) introduced a method to adjust the neutral stratification to buoyancy influenced atmospheric measurements;

$$U(z) = \frac{u_*}{\kappa} \left(\ln \frac{z}{z_o} - \psi(z/L) \right). \quad (5)$$

The stratification function, $\psi(z/L)$, is defined for stable conditions ($z/L > 0$) as;

$$\psi(z/L) = -5(z/L) \quad (6)$$

and for unstable conditions ($z/L > 0$) as;

$$\psi(z/L) = \ln \left(\frac{1+X^2}{2} \right) \left(\frac{1+X}{2} \right)^2 - 2 \tan^{-1} X + \pi/2 \quad (7)$$

$$X = (1 - 16(z/L))^{\frac{1}{4}} \quad (8)$$

where X is a fitted function (Panofsky and Dutton, 1984). The drag coefficient is defined as;

$$C_{DN}(z) = \frac{\tau}{\rho (U_{zN})^2} = \left(\frac{u_*}{U_{zN}} \right)^2 = \left[\frac{k}{\ln \left(\frac{z}{z_o} \right) - \psi(z/L)} \right]^2 \quad (9)$$

a term often used to parameterize the momentum flux.

3 Description of Experiment

The physics of air-sea momentum transfer in the coastal zone are significantly different compared to deep-water conditions. In deep-water, waves are dispersive and capable of reaching dynamic equilibrium with the wind. When the wind suddenly changes

speed or direction in deep-water, growth of young wind-waves (short wavelengths) can take as little as a few seconds with directions similar to the local wind (Jones and Toba, 2001).

Long wavelength or low frequency waves travel far from their point of origin and dissipate very little energy. As deep-water waves travel inshore at the USACE-FRF, the wave field refracts as the water depth decreases. Wave refraction prohibits the near-shore wave field from aligning with the local wind, generating asymmetric shear stresses. Nearshore waves at the USACE-FRF also experience shoaling, breaking and limited phase speed (governed by the local water depth), enhancing flow separation, atmospheric turbulence and drag (Jones and Toba, 2001; Ly and Benilov, 2002).

The USACE-FRF pier is oriented 70° north and the instruments, attached to two of the tower legs, point 40° north (Figure 3). Onshore winds originate between 340° through 160° north clockwise. Tower instruments sample at 10 Hz. Instrument measurements include: 3-D wind components (u, v, w), water vapor concentration (q) and sonic temperature (T_s) enabling the following parameters to be calculated: mean wind speed (U), mean wind direction ($^\circ$ north), mean air temperature (T), mean water vapor concentration (Q), 3-D turbulent wind fluctuations (u', v', w'), turbulent water vapor and temperature fluctuations (q', t'), turbulent temperature fluctuations (t'), friction velocity (u_*), scaling temperature (t_*) defined in Equation 10, scaling specific humidity (q_*) defined in Equation 11, atmospheric stability (z/L) and drag coefficient (C_D). Data were integrated through a data acquisition systems consisting of computer located in a NOAA shed near the end of the pier.

$$t_* = \frac{\overline{t'w'}}{k\sqrt{-\overline{u'w'}}} \quad (10)$$

$$q_* = \frac{\overline{q'w'}}{k\sqrt{-\overline{u'w'}}} \quad (11)$$

The eddy correlation method (ECM) is applied to calculate Reynolds stresses directly from covariance's from the parameters of interest (Large and Pond, 1981). Recorded data were processed according to the following procedure: extract timestamp, calculate mean parameters, calculate mean wind speed and direction, error (spike) checking, rotate wind velocities into the mean wind direction about the z-axis, calculate standard deviations, detrend variables, calculate covariance's, calculate scaling parameters, determine

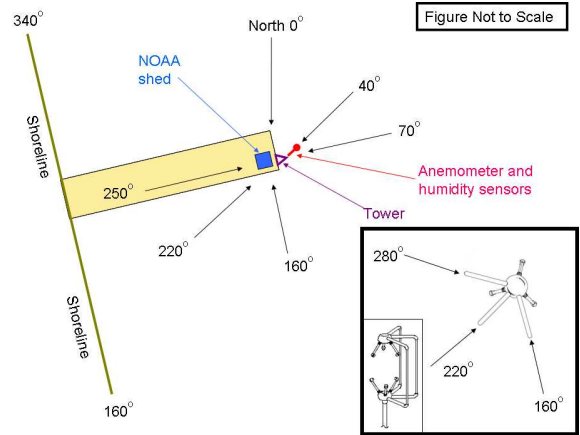


Figure 3: USACE-FRF pier schematic.

momentum flux direction, calculate stability parameters, perform stability corrections, compare drag coefficient results to historical expressions.

4 Results

USACE-FRF momentum data are highly unique due to: stable measurement platform, accessibility to instruments, availability of wave information from a nearshore cross-shore array measurement system, depth-limited wave conditions and coastal zone location. Data were collected over a twenty-seven (27) month period between October 2005 through December 2007, providing 18,927 30-minute data sets for analysis.

Measurements are standardized to 10-m height. Data sets with mean wind speeds less than 10 m/s measured at 16.7-m were excluded for the remainder of this analysis, reducing available data by over 90%. Additional screening involved removing obvious spectral signature errors and upwards momentum fluxes resulting in 924 30-minute data sets for investigation. Majority of the remaining data sets originate from the northeast direction (Figure 4).

Stability corrections increase or decrease the 10-m neutral wind speed depending if turbulence or buoyancy forces dominate (Figure 5). Positive and negative stability parameters (z/l) were predominantly measured from the offshore and onshore incident wind directions, respectfully (Figure 6). As the wind speed increases, stability corrections become minimal.

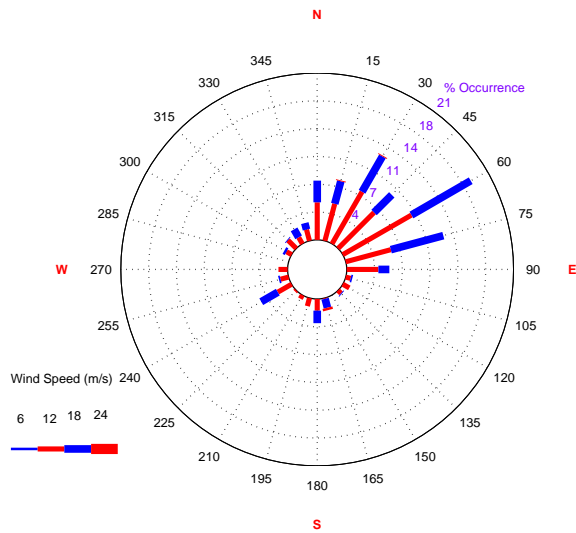


Figure 4: Wind rose indicating direction wind originates from.

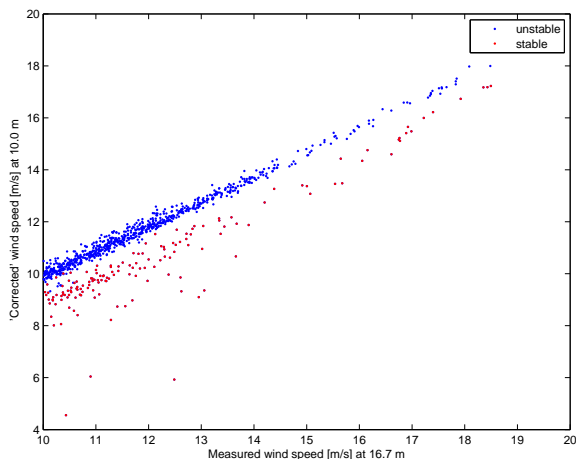


Figure 5: Impact of stability (temperature only) corrections on wind speed at 10-m.

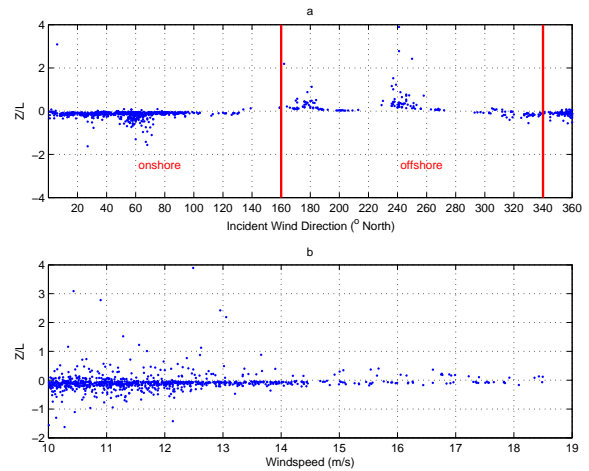


Figure 6: *a*) Monin-Obukhov length scale (z/L) at 10-m vs. incident wind direction; *b*) Monin-Obukhov length scale (z/L) at 10-m vs. measured wind speed.

Data are inspected to identify potential obstructions that influence measurements from certain incident wind directions (Friebel et al., 2009). Instrumentation geometry and supporting structures can increase or decrease the mean wind vector as flow obstructions generate shadow zones and turbulent wakes (Kaimal, 1979; Wyngaard, 1981). Vertical wind speeds, fluxes and drag coefficients are inspected for structure distortion and deviation from open ocean parameterizations.

The greatest wind speeds are expected from the northeast direction due to typical nor'easter storms that frequent the eastern seaboard. However, wind speeds and directions are not limited at the USACE-FRF research pier as storms may approach from any direction (Figure 4). Therefore, it is not possible to correlate data scattering of mean wind speed versus direction as an indicator of corrupted measurements.

Vertical wind speed

The mean vertical wind speed, W , is used as an indicator for corrupted wind measurements. Since the common processing routine rotating $W = 0$ is not employed, the data are able to be inspected to serve as an indicator for possible structure distortion. Vertical winds are averaged every 5-degrees and plotted versus incident wind direction (top of Figure 7). To eliminate wind speed bias, vertical winds are normalized

by the horizontal component (bottom of Figure 7).

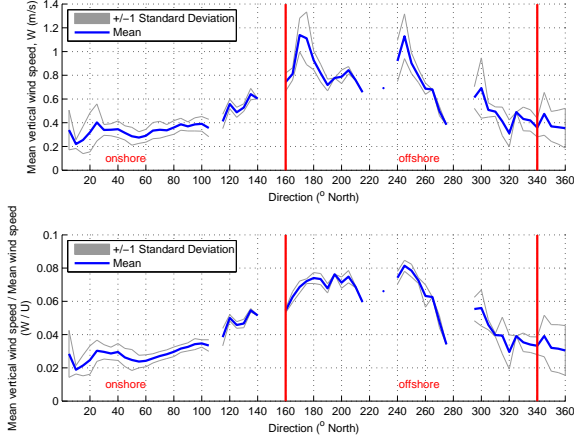


Figure 7: Incident wind direction vs. mean vertical wind, where offshore winds at the USACE-FRF originate clockwise between 160° through 340° north.

Reynolds momentum flux measurements are subject to flow distortion as fixed position instruments need to be oriented into the prevailing wind to minimize data corruption. Corrupted vertical winds are identified between 160° through 300° north. These directions correlate with directions expected to include influences of the instrumentation, supporting structures and development of an inner shoreline boundary layer (Figure 3). It should be noted that limited data are available for a number of wind directions (Figure 8), specifically for the corrupted directions identified above. There are five (5) potential sources to measure a mean vertical velocity in each measurement record: data sets are finite in length; boundary layer horizontal, non-uniformity due to aerodynamic roughness changes as the wind switches direction between the land to sea (Monin and Yaglom, 1975); formation of inner boundary layer in the nearshore as slower/steeper waves suppress the wind; misalignment or “tilt” of the anemometer; and structure distortion.

Friction velocity

To help interpret friction velocity measurements, covariance’s of $u'w'$ are plotted versus incident wind directions and normalized by the mean horizontal wind speed (top and bottom of Figure 9 respectfully). Every 1° of vertical tilt introduces a 6-9% error in the measured friction velocity (Wilczak et al., 2001).

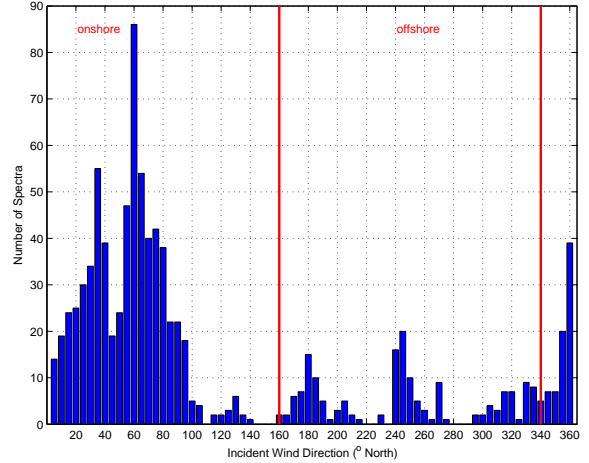


Figure 8: Number of data (spectra) available at each 5-degree band for this analysis.

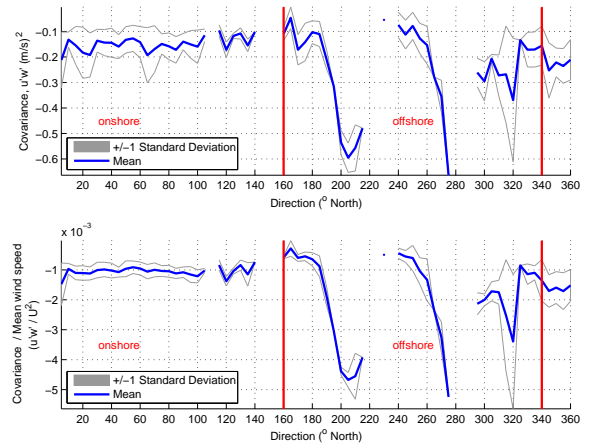


Figure 9: Incident wind direction vs. momentum flux ($u'w'$).

Significant deviation of $u'w'$ exists for clockwise measurements between 190° through 340° north, again correlating with previously identified distortion directions. The limited amount of data for these incident wind directions limits the statistical confidence of the results. If offshore measurements are removed, the friction velocity demonstrates a strong linear relationship with $1/29th$ of the neutral wind speed (Figure 10). As expected, the friction velocity peaks at neutral conditions ($z/L \rightarrow 0$) (Figure 11).

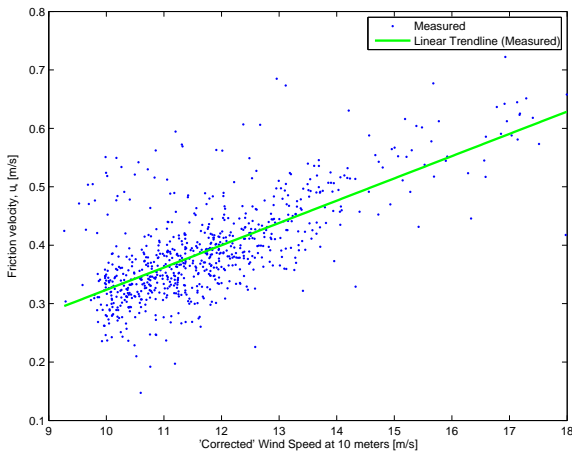


Figure 10: Measured friction velocity vs. 'corrected' wind speed at 10-m for onshore wind directions.

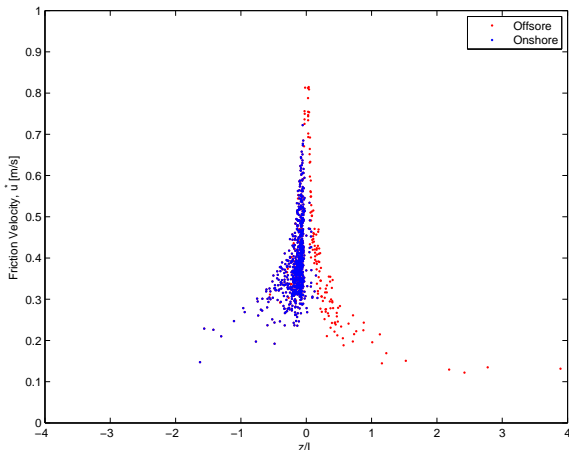


Figure 11: Friction velocity (u_*) vs. stability parameter (z/L).

Drag coefficient

Drag coefficients are calculated to determine dependence on wind speed and compared to historic open ocean parameterizations. Majority of air-sea momentum flux measurements collected for wind speeds up to 15 m/s demonstrate that as the wind speed increases, the drag coefficient also increases (Large and Pond, 1981; Smith, 1988). Higher drag coefficients are expected in depth-limited conditions (Resio, 1987, 1988; Geernaert, 1987; Smith et al., 1992; Jones and Toba, 2001). For the remainder of this analysis, only onshore measurements are considered. Drag coefficient measurements between 10 to 15 m/s demonstrate significant variability (Figure 12).

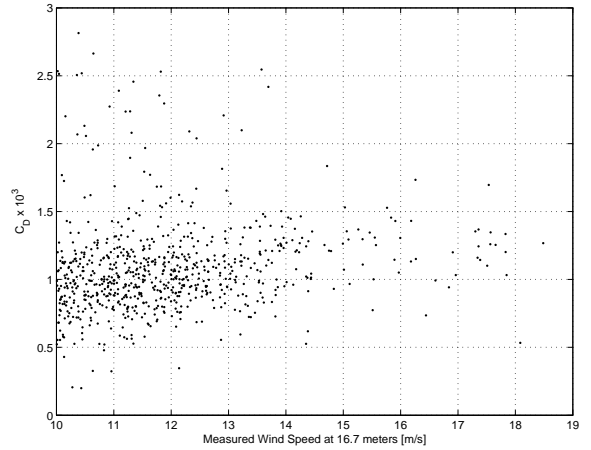


Figure 12: Drag coefficient measured at 16.7-m for onshore wind directions.

In an effort to understand the impacts of the coastal zone on the measured drag coefficient, onshore drag measurements are standardized to 10-m height and compared to historical open ocean parameterizations. Unexpectedly, drag coefficients measured at the USACE-FRF are lower than open ocean parameterizations (Figure 13). Drag coefficients are then partitioned in 30-degree bands to isolate orthogonal, semi-orthogonal and parallel winds to the underlying (assumed shore-parallel) wave field (Figure 14). As Figure 14 demonstrates, the largest drags are measured clockwise between $340^\circ - 10^\circ$ north (a compilation of over ten different wind events).

To compensate for the underlying surface current, the relative wind speed is calculated by subtracting the i and j component of the surface current from the wind. Measured drag coefficients will increase if the

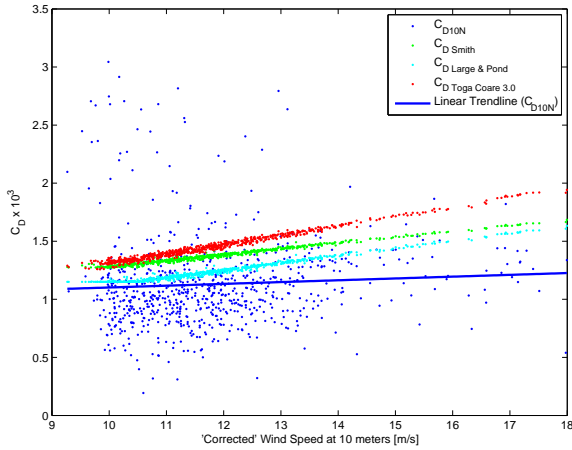


Figure 13: Drag coefficient for onshore wind directions (320° to 160° N) at 10-m.

relative U_{10} is less than the wind speed. Figure 15 illustrates that as strong northeast winds drive north to south currents, a smaller relative wind speed prevails for these directions. Applying the relative wind speed correction to all data, the difference between the historic and measured drag coefficients reduces, yet a significant offset still remains (Figure 16).

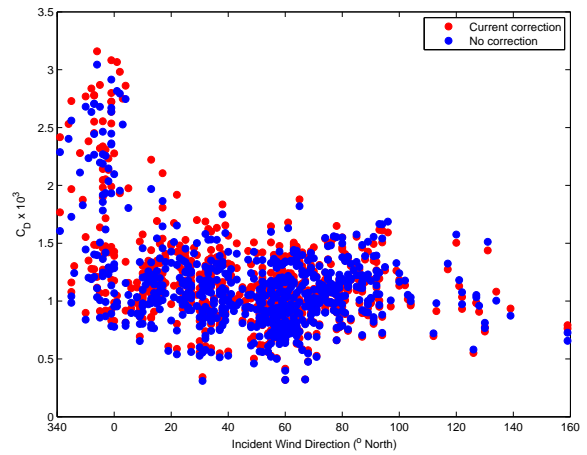


Figure 15: Relative wind speed correction on measured drag coefficient.

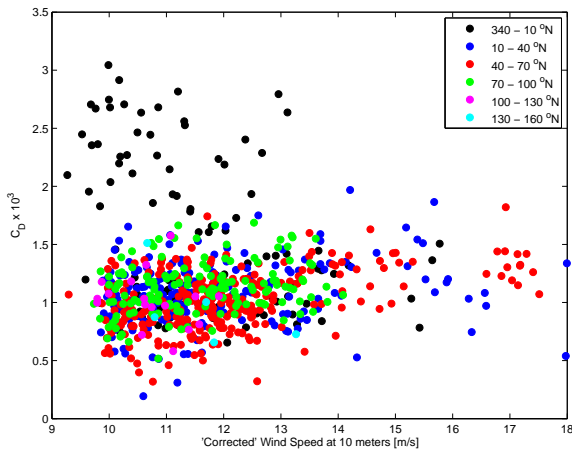


Figure 14: Partitioned drag coefficients vs. incident wind direction.

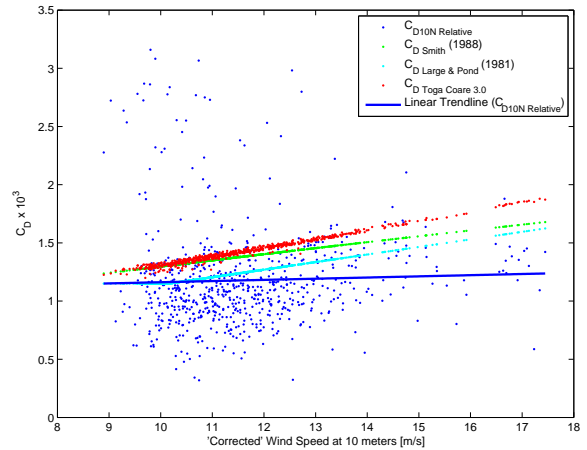


Figure 16: Drag coefficient for onshore wind directions (320° to 160° N) at 10-m.

5 Summary

The primary objective of this experiment is to gain a better understanding of the physics associated with drag coefficient behavior in the nearshore during extreme wind events. High-quality in-situ momentum flux data have been collected over the air-sea interface at the U.S. Army Corps of Engineers Field Research Facility pier in Duck, NC. This report describes tower momentum flux measurements collected at 16.7-m above mean sea level (MSL) from October 2005 through December 2007.

Air-sea momentum transfer in the nearshore is significantly different compared to open water, coastal wind and swell case measurements. In the open ocean, wave heights and directions are not constrained. Nearshore waves at USACE-FRF are depth-limited and subject to numerous coastal processes including refraction, shoaling and breaking. Waves are not always in equilibrium state, especially swell. Wave refraction prohibits the wave field from aligning with the local wind, producing asymmetric shear stresses. During extreme wind events, the surf zone expands seaward beyond the measurement tower, exposing flux measurements to wave breaking. Wave breaking enhances flow separation, resulting in increased atmospheric turbulence that, in turn, increases drag as additional momentum is transferred to the sea surface (Ly and Benilov, 2002).

Onshore drag coefficients calculated at the USACE-FRF are less than historical open ocean parameterizations. Measured drag coefficients do increase if the underlying surface current is taken into account; however, measurements are still less than historical parameterizations. Since the USACE-FRF anemometer measures $W \neq 0$, measurements are expected to under-estimate both the wind stress and drag. Unfortunately, the potential sources for an upward mean flow identified earlier in this paper limit the authors from performing a second rotation to remove the mean W . In addition, it is presently unknown why the largest drag coefficients are measured between $340^\circ - 10^\circ$ north. Two hypothesis are proposed for the higher $340^\circ - 10^\circ$ north drag coefficient trend: the anemometer is measuring structure distortion and/or cross-winds are unsteady for a portion of the time series.

Acknowledgements

The authors would like to thank Gerrit de Leeuw of the Finnish Meteorological Institute, Marcel Moer-

man of TNO Defence, Security and Safety and Chris Zappa of Columbia University for their help in establishing the tower measurement system. The authors are extremely grateful to both Kent Hathaway, Cliff Baron and Chuck Long of the U.S. Army Corps of Engineers Field Research Facility for their expert assistance with instrumentation, computers and numerous insightful discussions, respectfully. This project was made possible thanks to funding by the U.S. Army Corps of Engineers MORPHOS program.

References

- Charnock, H., 1955. Wind stress on a water surface. *Quarterly Journal of Royal Meteorology Society* 81, 639–640.
- de Leeuw, G., Moerman, M., Zappa, C. J., McGillis, W. R., 2007. Long-term measurements of drag coefficients and waves in high winds: winter 2006 results. Tech. rep.
- Donelan, M. A., 1990. *The Sea: Air-Sea Interaction*. Vol. 9. *Ocean Engineering Science*, pp. 239–292.
- Donelan, M. A., Drennan, W., Katsaros, K., 1997. The air-sea momentum flux in conditions of mixed wind sea and swell. *Journal of Physical Oceanography* 27, 2087–2099.
- Drennan, W. M., Graber, H. C., Hauser, D., Quentin, C., 2003. On the wave age dependence of wind stress over pure wind seas. *Journal of Geophysical Research* 108 (C3).
- Drennan, W. M., Kahma, K. K., Donelan, M. A., 1999. On momentum flux and velocity spectra over waves. *Boundary-Layer Meteorology* 92, 489–515.
- Friebel, H. C., Herrington, T. O., Benilov, A. Y., 2009. Evaluation of the Flow Distortion around the Campbell Scientific CSAT3 Sonic Anemometer Relative to Incident Wind Direction. *Journal of Atmospheric and Oceanic Technology* 26 (3), 548–558.
- Geernaert, G. L., 1987. On the importance of the drag coefficient in air-sea interaction. *Dynam. Atmos. Oceans* 11, 19–38.
- Grelle, A., Lindroth, A., 1994. Flow distortion by a solent sonic anemometer: wind tunnel calibration

- and its assessment for flux measurements over forest and field. *Journal of Atmospheric and Oceanic Technology* 11 (6), 1529.
- Hsu, S. A., 1988. *Coastal Meteorology*. Academic Press.
- Jones, I. S. F., Toba, Y., 2001. *Wind stress over the ocean*. Cambridge University Press.
- Kaimal, J. C., 1979. Sonic anemometer measurement of atmospheric turbulence. In: *Proceedings Dynamic Flow Conference*. pp. 551–565.
- Katsaros, K. B., Donelan, M. A., Drennan, W. M., 1993. Flux measurements from a swath ship in SWADE. *Journal of Maritime Systems* 4, 117–132.
- Large, W. G., Pond, S., 1981. Open ocean momentum flux measurements in moderate to strong winds. *Journal of Physical Oceanography* 11, 324–336.
- Ly, L., Benilov, A. Y., 2002. Surface waves. *Encyclopedia of Atmospheric Sciences I*, 118–127.
- Monin, A. S., Obukhov, A. M., 1954. The basic regularities of turbulent mixing in the atmospheric surface layer. *Tr. Akad. Nauk SSSR, Geofiz. Inst.* 24, 163–187.
- Monin, A. S., Yaglom, A. M., 1975. *Statistical fluid mechanics: mechanics of turbulence*. The MIT Press.
- Panofsky, H. A., Dutton, J. A., 1984. *Atmospheric Turbulence*. Wiley.
- Paulson, C. A., 1970. The mathematical representation of wind speed and temperature profiles in unstable atmospheric surface layer. *Journal Applied Meteorology* 9, 857–861.
- Prandtl, L., 1932. *Meteorologische Anwendung der Stromungslehre. Beitrge zur Physik der freien Atmos.* 19, 188–202.
- Resio, D. T., 1987. Shallow-water waves. I: Theory. *Journal of Waterway, Port, Coastal and Ocean Engineering* 113 (3), 264–281.
- Resio, D. T., 1988. Shallow-water waves. II: Data comparisons. *Journal of Waterway, Port, Coastal and Ocean Engineering* 114 (1), 50–65.
- Smith, S., 1988. Coefficients for Sea Surface Wind Stress, Heat Flux, and Wind Profiles as a Function of Wind Speed and Temperature. *Journal of Geophysical Research* 93 (C12), 15467–15472.
- Smith, S. D., 1980. Wind stress and heat flux over the ocean in gale force winds. *Journal of Physical Oceanography* 10, 709–726.
- Smith, S. D., Anderson, R. J., Oost, W. A., Kraan, C., Maat, N., de Cosmo, J., Katsaros, K. B., Davidson, K. L., Bumke, K., Hasse, L., Chadwick, H. M., 1992. Sea surface wind stress and drag coefficients: The hexos results. *Boundary-layer meteorology* 60, 109–142.
- Volkov, Y. A., 1970. Turbulent flux of momentum and heat in the atmospheric surface layer over a disturbed surface. *Izv., Atmospheric and Oceanic Physics Series* 6.
- Weiser, A., Fiedler, F., Corsmeier, U., October 2001. The influence of the sensor design on wind measurements with sonic anemometer systems. *Journal of Atmospheric and Oceanic Technology* 18 (10), 24.
- Wilczak, Oncley, Stage, 2001. Sonic anemometer tilt correction algorithms. *Boundary-Layer Meteorology* 99, 127–150.
- Wolf, A., Laca, E. A., 2007. Cospectral analysis of high frequency signal loss in eddy covariance measurements. *Atmospheric Chemistry and Physics Discussions*, 7, 13151-13173, 2007.
- Wyngaard, J. C., 1981. The effects of probe-induced flow distortion on atmospheric turbulence measurements. *Journal of Applied Meteorology* 20, 784–794.
- Wyngaard, J. C., Zhang, S. F., 1985. Transducer shadow effects on turbulence spectra measured by sonic anemometers. *Journal of Atmospheric and Oceanic Technology* 2, 548–558.